



Adsorption of dye crystal violet onto surface-modified *Eichhornia crassipes*

Sumanjit Kaur*, Seema Rani, Rakesh Kumar Mahajan

Department of Chemistry, Guru Nanak Dev University, Amritsar 143005, India
Tel. +91 183 2258802 09 Ext. 3455; email: sumangndu@yahoo.co.in

Received 10 September 2013; Accepted 12 October 2013

ABSTRACT

Eichhornia charcoal is modified with sodium dodecyl sulfate (SDS) is an anionic surfactant being employed as an adsorbent for the removal of dye crystal violet from aqueous solutions. Morphology and surface of the adsorbent were characterized by elemental analysis, Boehm titrations, point of zero charge measurements, Brunauer, Emmett, Teller, scanning electron microscope, FTIR and XRD techniques. Batch adsorption experiments were conducted to evaluate the effect of contact time, pH, initial dye concentration, temperature, adsorbent dose, and salt (NaCl) concentration. Adsorption mechanism of the dye for the adsorbent has been monitored through different kinetics and adsorption isotherm models. Positive value of change in entropy (ΔS) and change in enthalpy (ΔH) insinuated that adsorption process occurs with increase in randomness and endothermic, whereas negative values of free energy change (ΔG) signifies the spontaneous nature of the present system. It was alluded that kinetics followed a pseudo-second-order equation. On the basis of the Langmuir analysis, the maximum adsorption capacity was determined as 116.3 mg of dye per gram of adsorbent. Therefore, *Eichhornia crassipes*, a waste, modified by anionic surfactant was suitable to be used as an effective adsorbent for cationic dye removal.

Keywords: Crystal violet; *Eichhornia crassipes*; Sodium dodecyl sulfate; Adsorption; Kinetics; Thermodynamics

1. Introduction

Large quantities of dyes are used in different industries. It is estimated that about 10–15% of the dyes utilized in these industries are discharged into wastewater streams [1]. Contamination of water caused by organic pollutants is very dangerous due to their various side effects and carcinogenic nature [2]. Basic dyes used by the textile industry are the brightest class of soluble dyes. Their tinctorial value is very high: less than 1 ppm of the dye produces an obvious coloration [3]. However, cationic dyes are more toxic than anionic dyes [4]. Color removal from textile

wastewater is of major environmental concern because the discharge of colored wastewater into bodies of water can trigger many significant problems, including increasing toxicity and decreasing light penetration.

Various methods of dye/color removal, including aerobic and anaerobic microbial degradation, coagulation, chemical oxidation, membrane separation, electrochemical treatment, filtration, flocculation, softening, hydrogen peroxide catalysis, and reverse osmosis have been proposed from time to time [5–7]. Adsorption is generally considered to be an effective method for dye removal, and the most widely used adsorbent is activated carbon. However, it suffers from high cost of production and regeneration [8]. Various types of materials were, therefore,

*Corresponding author.

investigated as the possible alternatives, such as waste apricot, coconut shell, dairy sludge, bamboo grass, peat, orange peels, pea nut hulls, rice husk, ground nut shells charcoal and bagasse, jack fruit peels, date stone, and palm tree waste [9–21].

In this study, *Eichhornia crassipes* are used as an adsorbent, as it is available in plenty and people have been trying to remove the plant from many waterways, spending billions of dollars in doing so. This study involves the use of Eichhornia charcoal (EC) modified by anionic surfactant sodium dodecyl sulfate (SDS) for the removal of cationic dye crystal violet (CV) from aqueous solutions.

CV is also known as basic violet 3, gentian violet, and methyl violet 10B and it belongs to the class of triaryl methane dyes. It is well-known dye and has been used for various purposes such as a biological stain, a dermatological agent, a veterinary medicine, an additive to poultry feed to inhibit propagation of mold, intestinal parasites and fungus [22]. It is also extensively used in textile dyeing and paper coloration. It is a mutagen and mitotic poison [23]. The dye is responsible for causing moderate eye irritation, causing painful sensitization to light. It can cause permanent injury to the cornea and conjunctiva since the product contains a cationic dye and such dyes have been reported to cause toxicity to mammalian cells [24]. It may be absorbed in harmful amounts through the skin and cause skin irritation and digestive tract irritation. In extreme cases, it may lead to respiratory and kidney failure and permanent blindness [25]. Therefore, there are both environmental and health concerns on this particular dye. Hence, the removal of dye CV from aqueous solutions using surfactant modified Eichhornia charcoal (EC-SDS) has been investigated. Biosorption was carried out in the batch process including number of variables such as pH, concentration of the dye, biosorbent load, time, temperature, and ionic effect. Kinetic, equilibrium, and thermodynamic studies have also been conducted.

2. Materials and methods

2.1. Adsorbate

CV used in this study was of commercial quality (CI 42555, MF: $C_{25}H_{30}N_3Cl$, MW: 407.98, λ_{max} : 580 nm). Its IUPAC name is N-[4-[bis [4-dimethylamino)-phenyl]-methylene]-2, 5-cyclohexadien-1-ylidene]-N methyl methanaminium chloride. Structure of the dye used in this study is given in Fig. 1. Stock solution ($1,000 \text{ mg L}^{-1}$) was prepared by dissolving accurately weighed quantity of the dye in double-distilled water. Experimental dye solution of different

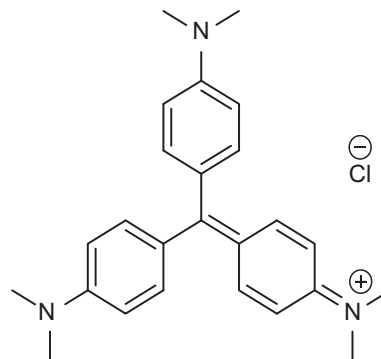


Fig. 1. Structure of dye CV.

concentrations was prepared by diluting the stock solution with suitable volume of double-distilled water. The initial solution pH was adjusted using 0.1 M HCl and 0.1 M NaOH solutions.

2.2. Adsorbent

Eichhornia leaves were collected from a pond at Ram Tirath Road, Amritsar (India). Eichhornia is available in plenty in India and also considered as one of the worst weed in the world. *E. crassipes* (Water hyacinth) is a free-floating aquatic plant well known for its production abilities. Collected material was washed several times with normal tap water followed by distilled water to eliminate earthy matter and all the soil particles. It were dried in the sun for two weeks and then in oven at 60°C for 12 h. EC was prepared in a very economical way by burning the cleaned material in the muffle furnace at 600°C at the rate of 10°C per minute for 2 h. Charcoal was sieved through sieves having mesh number 270 to remove coarse particles, and the corresponding particle size of $53 \mu\text{m}$ was obtained [26].

An anionic surfactant, sodium dodecyl sulfate (SDS, $\text{NaC}_{12}\text{H}_{25}\text{SO}_4$), 99% pure purchased from Sigma was used to modify the surface of EC. 30 g EC was kept in 100 mL of 10^{-2} M SDS solution for overnight with constant stirring at room temperature. The material (EC-SDS) was separated from the mixture by filtration, washed with distilled water, and dried at 100°C for 6 h. SDS modification covered the EC surface with negative charges and increased electrochemical interaction between dye molecules and the EC surfaces; therefore, increases the adsorption capacity.

2.3. Characterization techniques

FTIR spectra of the samples were recorded in a Perkin Elmer FTIR spectrophotometer in the range of

400–4,000 cm^{-1} taking KBr as the reference. Surface morphology was studied by scanning electron microscopy (Carl Zeiss Supra 55), equipped with EDX analyzer. The SEM analysis was carried out by gold sputtering process. The materials are further characterized by using the X-ray diffraction in the scanning mode on an XRD 7000 (Shimadzu, Japan) analytical instrument operated at 40 KV and a current of 30 mA with Cu-K α radiation ($\lambda = 1.5406 \text{ \AA}$). A Quantasorb Model QS-7 surface analyzer was used to calculate the surface area of the adsorbent particles.

The pH of zero point charge (pH_{zpc}) plays an important role in the adsorption process. The pH_{zpc} of adsorbent EC-SDS was determined by the reported method [27]. For this purpose, 50 mL of a 0.01 M sodium chloride (NaCl) solution was placed in a 100-mL Erlenmeyer flask. The pH was then adjusted to successive initial values between 2 and 12, by using either sodium hydroxide or hydrogen chloride (0.1 N), and 0.15 g of adsorbent was added to the solution. After a contact time of 24 h, the final pH was measured and plotted against the initial pH. The pH at which the curve crosses the line $\text{pH}(\text{final}) = \text{pH}(\text{initial})$ is taken as the pH_{zpc} . The pH of the EC-SDS was also measured in distilled water suspension. Surface chemistry was determined using Boehm titration methods [28]. Different batches of 100 mg EC-SDS were brought into contact with 50 mL solutions of 0.01 M NaHCO_3 , 0.01 M Na_2CO_3 , 0.01 M NaOH, and 0.01 M HCl. The mixtures were retained in a mechanical agitator at 100 rpm and 25°C for 24 h. Then, the aliquots were back-titrated with either 0.01 M HCl for acidic groups or 0.01 M NaOH for basic groups. Neutralization points were observed using two universal pH indicators, that is, phenolphthalein for the titration of strong base with strong acid, and methyl red for weak base with strong acid. The amount of each functional group was calculated with assumptions that NaHCO_3 neutralizes only carboxylic groups, Na_2CO_3 neutralizes carboxylic and lactonic groups, and NaOH neutralizes carboxylic, lactonic and phenolic groups, while HCl neutralizes basic groups [28].

2.4. Batch adsorption experiment

The batch adsorption experiments were conducted by taking 50 mL of dye solution with 50 mg of EC-SDS. For each test, the mixture was agitated at 150 rpm in a rotary Metrex water bath orbital shaker. Solutions were withdrawn at different time intervals and filtered using Whatman filter paper. The supernatants were used for dye concentration analysis. All the dye adsorption experiments were conducted in triplicate, and the average values were recorded. The

amount of dye adsorbed (q_t) per unit EC-SDS (mg dye per g adsorbent) was calculated according to a mass balance on the dye concentration using equation $q_t = V(C_o - C_t)/m$, where C_o is the initial dye concentration (mg L^{-1}), C_t is the dye concentration in solution (mg L^{-1}) at time t , V is the volume of the solution (L), and m is the mass of the adsorbent (g). The percent removal (%) of dye was calculated using the equation:

$$\% \text{ removal} = [(C_o - C_e)/C_o] \times 100$$

where C_e is the equilibrium concentration (mg L^{-1}).

2.5. Effect of adsorption parameters

To examine the effect of temperature, adsorption experiments were conducted at 30, 40, and 50°C, respectively. The influence of the initial pH was observed by adjusting the pH value of the dye solutions to 2, 4, 6, 8, 10, and 12 by using 0.5 M HCl or 0.5 M NaOH prior to the experiments. Sodium chloride was used to investigate the effect of salt on adsorption process.

3. Results and discussion

3.1. Characterization of adsorbent EC-SDS

The element analysis of EC-SDS shows 33% carbon, 2.7% nitrogen, 1.93% hydrogen and no sulfur contents. Total basic groups and total functionalized groups obtained by Boehm titration are 0.005 and 0.009 mM g^{-1} , respectively. The value of pH_{zpc} and pH for EC-SDS is 7.95 and 8 respectively. The Brunauer–Emmett–Teller (BET) surface area, total pore volume: and molecular cross sectional area was 68.77 $\text{m}^2 \text{ g}^{-1}$, 0.0346 $\text{m}^3 \text{ g}^{-1}$, and 0.162 nm^2 , respectively. The particle size of EC-SDS was found to be in the range of 0.47–1.5 μm .

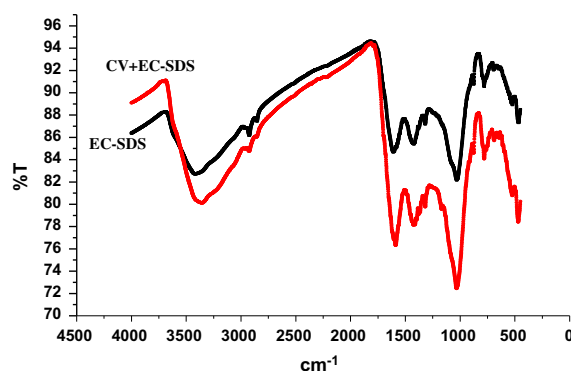


Fig. 2. FTIR spectra of adsorbent EC-SDS and dye loaded EC-SDS.

The sharp peak in the X-ray diffraction study of EC-SDS indicates the crystalline nature of the material. It is seen that there is no significant difference for XRD profiles of EC-SDS and CV-EC-SDS (figure not shown), but dye-loaded EC-SDS sample presents higher intensity of diffraction peaks. The results suggested that the dye-loaded EC-SDS is not inducing bulk phase changes.

The adsorbent EC-SDS was also characterized using the Fourier transform infra-red spectrophotometer before and after the adsorption of CV (Fig. 2). The adsorbent EC-SDS shows major peaks at 3,420, 1,609, 1,421, 1,031, and 780 cm^{-1} , respectively. The peak around 3,420 and 3,349 cm^{-1} represented the O–H stretching vibration that shows the presence of free hydroxyl group on the surface of EC-SDS. This vibration corresponded to inter- and intra-molecular hydrogen bonding among the constituents of biomass. Region in between 1,475 and 1,600 is due to C=C (aromatic), and 1,350–1,000 cm^{-1} for C–N stretching. After adsorption, CV-loaded EC-SDS the intensity of the peaks get shifted toward low-frequency and low-intensity region.

3.2. SEM study

The morphology of adsorbent EC-SDS was studied using a scanning electron microscope (SEM). The scanning electron micrographs enable the direct observation of the surface microstructures of the adsorbent material. Fig. 3 illustrated that adsorbent EC-SDS has considerable numbers of pores, and hence, there is a good possibility for dye to be trapped and adsorbed into these pores.

3.3. Effect of contact time and initial concentration

Contact time and initial concentration of adsorbate species have significant effect on adsorption and are

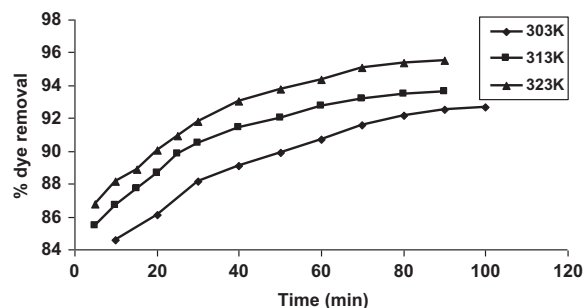


Fig. 4. Effects of contact time and temperature on percentage dye removal (adsorbent dose = 1 g L^{-1} , $C_0 = 20 \text{ mg L}^{-1}$, $\text{pH} = 8$).

important parameters for economical wastewater treatment application. Results reflected that dye removal increases with increase in contact time. Adsorption of dye was rapid for first 10 min; thereafter, it continued at a slower rate and finally reached equilibrium as a result of saturation of EC-SDS surface sites. It is also clear from Fig. 4 that the graphs are single and smooth, indicating monolayer coverage of the adsorbent surface by CV. The contact time decreases with increase in temperature. The increase in adsorption with increasing temperature indicates the endothermic nature of the dye adsorption onto adsorbent EC-SDS. Fig. 5 revealed that percentage removal increases with decrease in the initial concentration of dye CV on all the studied temperatures. At lower concentrations, all dye molecules present in the solution interact with the binding sites of the biosorbent, facilitating about 94% biosorption. However, all biosorbents have a limited number of binding sites, which become saturated at a certain concentration. Hence, at higher concentrations, more dye molecules are left unadsorbed in the solution due to the saturation of binding sites resulting in decreased biosorption efficiency. Similar results were reported by other workers also [25].

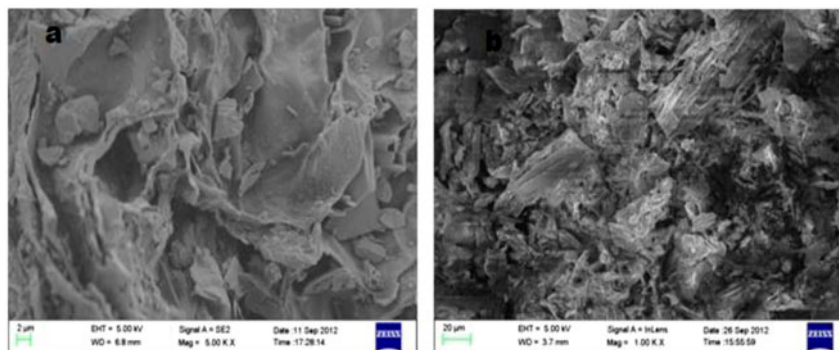


Fig. 3. SEM of EC-SDS and dye loaded EC-SDS.

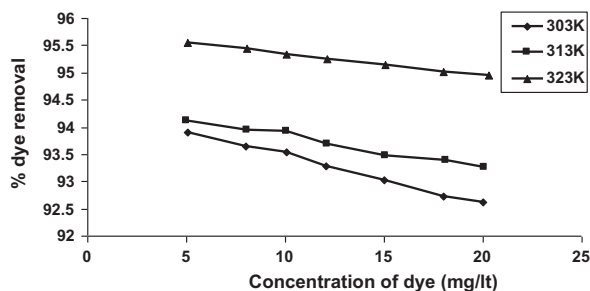


Fig. 5. Effect of initial concentration of dye CV on percentage dye removal by EC-SDS (adsorbent dose = 1 g L^{-1} , pH=8, equilibrium time 100 min).

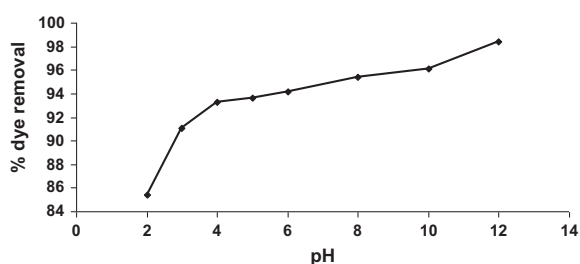


Fig. 6. Effects of pH on the adsorption of dye CV by EC-SDS. (adsorbent dose = 1 g L^{-1} , $C_o = 20 \text{ mg L}^{-1}$, temperature 313 K, and equilibrium time 100 min).

3.4. Effect of pH

The pH is the most important factor affecting the nature of the surface charge of the adsorbent, ionization of dye, and the extent and rate of adsorption capacity. The change of adsorption as a function of pH is shown in Fig. 6 at an initial concentration 20 mg L^{-1} and adsorbent dose 1 g L^{-1} . The pH of the adsorbent in aqueous solution was found to be 7.95 and zero point charge (pH_{ZPC}) of EC-SDS was 8.00. With increase in pH from 2 to 10, removal efficiency increases from 85 to 98.3%. It is attributed to the

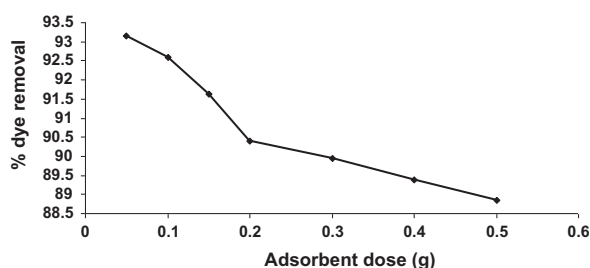


Fig. 7. Effect of EC-SDS dosage on dye removal ($C_o = 20 \text{ mg L}^{-1}$, temperature 313 K, pH=8 and equilibrium time 100 min).

electrostatic attraction between the negatively charged adsorption site and the positively charged dye molecules. At lower pH, the H^+ ions will compete with dye cations causing decrease in the adsorption.

3.5. Effect of adsorbent dose

Fig. 7 denotes the influence of EC-SDS on the adsorption of CV while keeping initial concentration and pH constant. It is seen that with increase in the amount of the adsorbent the dye removal decreases. It is to be ascribed to higher concentration of SDS leads to the formation of surfactant micelles in which dye is incorporated, thus preventing the dye being adsorbed onto the adsorbent surface hence adsorption decreases. Similar results were reported by other researchers [29].

3.6. Effect of salt

Most dye wastewater contains salts, and adsorption was found to be influenced by the concentration and nature of these ionic species [30]. Fig. 8 illustrates the effect of NaCl on the adsorption of dye CV on EC-SDS. Theoretically, when the electrostatic forces between the adsorbent surface and adsorbate ions are attractive, an increase in ionic strength will decrease the adsorption capacity. The facilitation for dyes adsorption in the presence of salts in aqueous solution could be produced by two mechanisms [31,32]. One is the addition of salts resulting in the dimerization of dyes in solution and rendering the molecule volume both smaller and more hydrophobic, which is favorable for adsorption process. With the addition of NaCl, the intermolecular forces between dye molecules, such as van der Waals forces, ion-dipole forces and dipole-dipole forces increase, and consequently, the repulsion forces among the negatively charged functional groups of dyes decrease, which results in

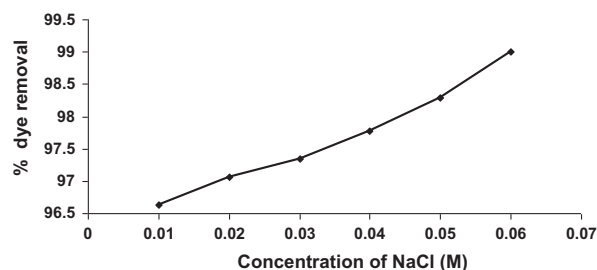


Fig. 8. Effect of solution ionic strength on the extent of dye adsorption ($C_o = 20 \text{ mg L}^{-1}$, temperature 313 K, and equilibrium time 100 min).

the dimerization of dyes in solution [31]. Furthermore, the other mechanism is the increase in ionic strength causing the compression of the diffuse double layer on the adsorbent, which facilitates the electrostatic attraction and contributes to the adsorption consequently [32].

3.7. Kinetics study

To clarify the adsorption process, several adsorption models considered are Lagergren's pseudo-first-order and pseudo-second-order kinetic model, intra-particle diffusion, Elovich and Bangham's model.

3.7.1. Pseudo-first-order equation

This equation is expressed as

$$\log(q_e - q_t) = \log q_e - \frac{k_f}{2.303} t \quad (1)$$

where q_e (mg g^{-1}) and q_t (mg g^{-1}) are the adsorption capacity at equilibrium and at time t , respectively, k_f (min^{-1}) is the rate constant of pseudo-first-order adsorption model. Plot of $\log(q_e - q_t)$ vs. t (not shown) gives a straight line and values k_f and R^2 are obtained (Table 1). The first-order kinetics is considered to be valid if values of q_e from the intercept of the Lagergren plot and from experiments are comparable. In this study, the value of q_e (calculated) obtained by first-order model does not match with the experimental value ($q_{e, \text{exp}}$, experimental), so there is the need of pseudo-second-order kinetic model.

3.7.2. Pseudo-second-order

Lagergren equation is given as follows:

$$\frac{t}{q_t} = \frac{1}{k_s q_e^2} + \frac{1}{q_e} t \quad (2)$$

where k_s is the rate constant of pseudo-second-order adsorption ($\text{g mg}^{-1} \text{min}^{-1}$). Table 1 contained the values of rate constant (k_s), the equilibrium adsorption capacity (q_e), and the correlation coefficients (R^2). The linear regression correlation coefficient reached to 0.999 for the pseudo-second-order kinetic model. Moreover, the calculated equilibrium adsorption amount ($q_{e, \text{cal}}$) was also much closer to the experimental values. ($q_{e, \text{exp}}$) in the pseudo-second-order kinetic

Table 1

Values of kinetic parameters for the adsorption of CV onto EC-SDS at various temperatures (adsorbent dose = 1 g L^{-1} , $C_o = 20 \text{ mg L}^{-1}$, pH = 8, equilibrium time = 100 min)

Equations	Parameters	Temperature (K)		
		303	313	323
Pseudo first order	q_e exp (mg g^{-1})	18.41	18.59	18.99
	q_e cal (mg g^{-1})	3.14	2.26	3.15
	k_f (min^{-1})	0.037	0.042	0.049
	R^2	0.92	0.98	0.94
Pseudo-second-order	q_e exp (mg g^{-1})	18.41	18.59	18.99
	q_e cal (mg g^{-1})	18.76	18.86	19.19
	k_s ($\text{g mg}^{-1} \text{min}^{-1}$)	0.0248	0.0387	0.0398
	R^2	0.99	0.99	0.99
Intra-particle diffusion	k_{id} ($\text{mg g}^{-1} \text{min}^{-0.5}$)	0.283	0.288	0.292
	C (mg g^{-1})	15.77	16.26	16.61
	R^2	0.99	0.98	0.97
	Elovich	a	5.88×10^7	1.55×10^{10}
Bangham	b	1.23	1.52	1.55
	R^2	0.97	0.98	0.99
	k_o (g)	60.02	67.26	74.89
	α	0.16	0.15	0.14
	R^2	0.96	0.98	0.99

model. Therefore, it has been concluded that the pseudo-second-order adsorption model is more suitable for describing the adsorption kinetics of CV on EC-SDS.

3.7.3. An intraparticle diffusion model

Based on the theory proposed by Weber and Morris [33] was employed to identify the diffusion mechanism. The effect of intra particle diffusion resistance on adsorption can be evaluated by the following equation:

$$q_t = k_{id} t^{1/2} + C \quad (3)$$

where k_{id} is the rate constant of intra particle diffusion ($\text{mg g}^{-1} \text{min}^{-0.5}$), and C gives the information regarding the thickness of boundary layer. Values of k_{id} and correlation coefficient are listed in Table 1. Adsorption process comply with two phases: the initial curved portion of the plot was due to surface adsorption and rapid external diffusion, indicating a boundary layer effect while the second linear portion was due to

intraparticle diffusion [34]. The linear portion of the curves does not pass through the origin suggesting that the mechanism of CV removal on EC-SDS is complex and both the surface adsorption and intraparticle diffusion contributes to the adsorption process.

3.7.4. Elovich model

This model is a general application of chemisorptions kinetics, assumes that the active sites of adsorbents are heterogeneous and exhibit different activation energies for the adsorption of organic compounds [35]. Elovich model is expressed by the following equation;

$$q_t = \frac{1}{b} \ln(ab) + \frac{1}{b} \ln t \quad (4)$$

where a and b are constants. The constant a is considered as the initial sorption rate ($\text{mg g}^{-1} \text{min}^{-1}$), and b is related to the extent of surface coverage and activation energy for chemisorptions (g mg^{-1}). The values of these constant with their correlation coefficient (R^2) are presented in Table 1.

Kinetic data were further costumed to know about the slow step occurring in the present adsorption system using *Bangham's equation* [36].

$$\text{Log log } (C_o / (C_o - q_t m)) = \text{log } (k_o m / 2.303V) + \alpha \text{log } t \quad (5)$$

where C_o is the initial concentration of dye in solution (mg L^{-1}). V is the volume of the solution (mL), m is the weight of adsorbent per liter of solution (g L^{-1}). q_t (mg g^{-1}) is amount of dye adsorbed at time t and α (<1) and k_o are constants and are accommodated in Table 1. Linear plot ($\text{Log log } (C_o / C_o - q_t m)$ vs. $\text{log } t$) demonstrated that the diffusion of adsorbate into pores of adsorbents is not the only rate-controlling step [37].

3.8. Rate expression and treatment of data

For wastewater treatment, the rate at which dissolved organic substances are removed from dilute aqueous solutions by solid adsorbents is an extremely significant aspect and the mechanism of the involved process also plays an equally important role. Thus, to identify whether the rate determining step of the enduring process is particle diffusion or film diffusion, the mathematical treatment prescribed by Boyd et al. [38] and Richenberg [39] was applied and various parameters were calculated by using the following equations:

$$F = 1 - \frac{6}{\Pi^2} \exp(-Bt) \quad (6)$$

where F is the fractional attainment of equilibrium at time t , and B_t is a mathematical function of F . The F is acquired as $F = q_t / q_e$, where q_t (mg g^{-1}) and q_e (mg g^{-1}) are amounts adsorbed after time t and at equilibrium time, respectively. Substituting F into Eq. (6), the kinetic expression becomes:

$$B_t = -0.4977 - \ln\left(1 - \frac{q_t}{q_e}\right) \quad (7)$$

From the plot of B_t vs. time (Fig. 9), the process was classified as a film diffusion or particle diffusion-controlled mechanism. If a plot of B_t vs. t is a straight line passing through the origin, then adsorption will be governed by a particle-diffusion mechanism, otherwise governed by film diffusion [8]. It is necessary to point out here that film diffusion is observed when external transport of the ingoing ions is greater than internal transport, where as particle diffusion governs the rate, when external transport is less than internal transport [25]. Fig. 9, (B_t vs. time) gives straight lines not passing through the origin at all temperatures, suggesting that the rate-determining process is film diffusion.

3.9. Adsorption isotherm

Adsorption isotherms provide important models in the description of adsorption behavior, indicating the interaction of the adsorbate with adsorbents and variation of adsorption uptakes with adsorbate concentrations at given pH and temperature. Sorption equilibrium studies at different temperatures (30, 40,

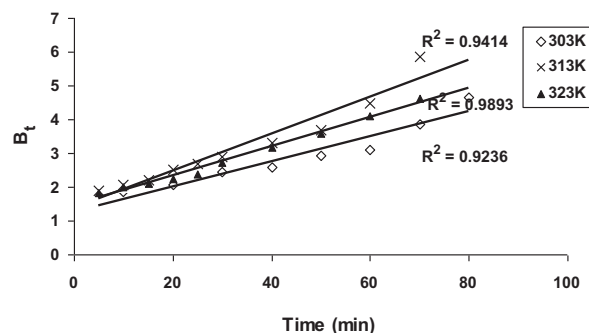


Fig. 9. Correlationship of B_t vs. time (min) on the adsorption of CV onto EC-SDS at different temperatures (EC-SDS dose=1 g L^{-1} , $C_o = 20 \text{ mg L}^{-1}$, pH=8.0).

50°C) were conducted by batch technique. Relation between the amount of dye adsorbed by a unit weight of adsorbent and remaining concentration of the dye in the solution is described by various forms of adsorption isotherms [40]. In this study, Langmuir, Freundlich and Tempkin, non-ideal competitive adsorption (NICA) model and Dubinin–Radushkevich isotherms were employed to investigate the adsorption behavior of dye CV onto EC-SDS.

3.9.1. Langmuir isotherm model

This model is proposed by Langmuir is based on the assumption that adsorption occurs at specific homogenous sites within the adsorbent. It explains monolayer adsorption which lies on the fact that the adsorbent has a finite capacity for the adsorbate, that is, at equilibrium; a saturation point is attained where no further adsorption can occur. The linear equation this model is represented as follows:

$$\frac{C_e}{q_e} = \frac{C_e}{C_m} + \frac{1}{K_L C_m} \quad (8)$$

where q_e is the amount of dye adsorbed per unit weight of adsorbent (mg g^{-1}), C_e is the equilibrium concentration of dye in the bulk solution (mg L^{-1}), C_m is the monolayer adsorption capacity (mg g^{-1}), and K_L is Langmuir constant. Basically, it is the reciprocal value of the concentration at which half the saturation of the adsorbent is reached. Maximum adsorption capacity (C_m) was found to be 116.3 mg g^{-1} (Table 2), and it is quite high in comparison with EC without modification [41].

The essential characteristic of a Langmuir isotherm can be expressed in terms of a dimensionless constant separation factor, R_L . The Langmuir adsorption constant K_L (L mg^{-1}) can be used to determine a dimensionless separation factor R_L , defined by the equation, $R_L = 1/(1+K_L C_o)$, where C_o is the initial concentration (mg L^{-1}). The value of parameter R_L indicates the nature of the adsorption process [42] (1) $R_L > 1$ for unfavorable adsorption, (2) $R_L = 1$ for linear adsorption, (3) $0 < R_L < 1$ for favorable adsorption, and (4) $R_L = 0$ for irreversible adsorption. R_L value decreased with the increase in C_o . The value of R_L at temperatures 30, 40, and 50°C were found to be 0.22, 0.21, and 0.20, respectively. Values of R_L are greater than zero and less than unity, alluded that Langmuir isotherm is favorable for adsorption of CV on EC-SDS.

Table 2

Isotherm constants for adsorption of CV onto EC-SDS at different temperatures (adsorbent dose = 1 g L^{-1} , $C_o = 20 \text{ mg L}^{-1}$, pH = 8, equilibrium time = 100 min)

Equations	Parameters	Temperature (K)		
		303	313	323
Langmuir	K_L (L mg^{-1})	0.178	0.186	0.193
	C_m (mg g^{-1})	88.49	92.59	116.27
	R^2	0.95	0.96	0.99
	K_F (mg g^{-1}) (L mg^{-1}) ^{1/n}	13.26	14.42	19.02
Freundlich	n	1.14	1.12	1.09
	R^2	0.99	0.99	0.99
	K_T (L mg^{-1})	4.40	4.79	6.33
Tempkin	B_1	9.21	9.44	9.66
	R^2	0.98	0.97	0.97
	N	1.06	0.99	0.99
Hill	K_G (mg L^{-1})	5.65	5.39	5.18
	R^2	0.99	0.99	0.99
Dubinin– Radushkevich	q_s (mg g^{-1})	20.98	21.14	22.03
	E (kJ M^{-1})	2.23	2.23	2.5
	R^2	0.97	0.98	0.96

3.9.2. Freundlich isotherm

It assumes heterogeneous surface energy for which the energy term in the Langmuir equation varies as a function of surface coverage. The well-known logarithmic form of the Freundlich isotherm is expressed by the following equation:

$$\log q_e = \log K_F + \frac{1}{n} \log C_e \quad (9)$$

K_F is the Freundlich adsorption constant related to the adsorption capacity of the adsorbent ($\text{mg}^{1-1/n} \text{ L}^{1/n} \text{ g}^{-1}$) and n , a dimensionless constant, which can be used to explain the extent of adsorption and the adsorption intensity between the solute concentration and adsorbent, respectively. The values of K_F and n obtained from the slope and intercept of the linear plot of $\log q_e$ vs. $\log C_e$ (figure not shown) are given in Table 2. The larger value of K_F with increase in temperature suggests enhanced adsorption at high temperatures and indication of the endothermic nature of the adsorption process.

3.9.3. Tempkin and Pyzhev

Tempkin and Pyzhev [43] considered the effects of indirect adsorbate–adsorbate interactions on adsorption isotherms. They reported that the heat of adsorption of

all the molecules on the adsorbent surface layer would decrease linearly with coverage due to adsorbate–adsorbate interactions. The linear form of this isotherm can be given by

$$q_e = B_1 \ln K_T + B_1 \ln C_e \quad (10)$$

K_T and B_1 are the Tempkin isotherm constants. The constant B_1 is related to the heat of adsorption. A plot of q_e vs. $\ln C_e$ enables one to determine the constants K_T and B_1 . These constants are included in Table 2. Increasing trend of value of B_1 indicates the endothermic nature of adsorption process.

3.9.4. NICA model

The model assumes that adsorption is a cooperative phenomenon, with the ligand-binding ability at one site on the macromolecule, may influence different binding sites on the same macromolecule [44,45].

The linear form of the Hill equation is:

$$\ln((q_{\max}/q_e) - 1) = \ln K_G - N \ln C_e \quad (11)$$

where K_G is the saturation constant (mg L^{-1}), N is the Hill cooperativity coefficient of the binding interaction, $N > 1$, positive cooperativity in binding, $N = 1$, noncooperative or hyperbolic binding, $N < 1$, negative cooperativity in binding. q_{\max} is the maximum adsorption capacity of the adsorbent (mg g^{-1}). q_e (mg g^{-1}) and C_e (mg L^{-1}) are the equilibrium dye concentrations in the solid and liquid phase, respectively. The values of K_G and N are represented in Table 2. The value of N in this study is near to unity reflects non cooperative binding of adsorbent with adsorbate. The value of saturation constant (K_G) also decreases with increase in temperature that reveals the speedy saturation at higher temperature.

3.9.5. The D-R isotherm equation

This is more general than the Langmuir isotherm because it does not assume a homogeneous surface or constant adsorption potential. It was applied to distinguish between the physical and chemical adsorption of dye [46]. The linear form of the Dubinin-Radushkevich isotherm can be given as

$$\ln q_e = \ln q_s - B\epsilon^2 \quad (12)$$

where q_s is D–R constant and can be correlated as

$$\epsilon = RT \ln(1 + 1/C_e) \quad (13)$$

where q_s is the maximum amount of adsorbate that can be adsorbed on adsorbent, the constant B gives the mean free energy E of sorption per molecule of sorbate when it is transferred to the surface of the solid from the bulk solution and can be computed using the following relationship:

$$E = 1/(2B)^{1/2} \quad (14)$$

The calculated D–R constant are provided in Table 2. Mean adsorption energy calculated from D–R isotherm gives an idea about the chemisorptions or physisorption. For $E < 8 \text{ kJ M}^{-1}$, physisorption control the adsorption mechanism, while a value between 8 and 16 kJ M^{-1} indicates involvement of chemisorptions process. Value of E for this study was found to be less than 8 kJ M^{-1} , suggesting that physisorption is responsible for the present adsorption process.

3.10. Error analysis

Applicability of the isotherm equations was compared by judging the correlation coefficients and the error analysis. Five different error functions were employed in this study to find out the most suitable isotherm model to represent the experimental data.

3.10.1. The sum of the squares of the errors

This error function, sum of the squares of the errors (SSE), is given as:

$$\text{SSE} = \sum_{i=1}^n (q_{e,\text{calc}} - q_{e,\text{exp}})_i^2 \quad (15)$$

Here, $q_{e,\text{cal}}$ and $q_{e,\text{exp}}$ are, respectively, the calculated and the experimental value of the equilibrium adsorbate solid concentration in the solid phase (mg g^{-1}) and n is the number of data points. This is the most commonly used error function [47].

3.10.2. The sum of the absolute errors (SAE)

SAE is given as follows:

$$\text{SAE} = \sum_{i=1}^n (|q_{e,\text{calc}} - q_{e,\text{exp}}|)_i \quad (16)$$

Isotherm parameters determined using the sum of the absolute errors (SAE) method provides a better fit as the magnitude of the errors increases, biasing the fit toward the high concentration data [47].

3.10.3. The average relative error

Average relative error (ARE) is given as:

$$\text{ARE} = \frac{100}{n} \sum_{i=1}^n \left| \frac{q_{e,\text{calc}} - q_{e,\text{exp}}}{q_{e,\text{exp}}} \right|_i \quad (17)$$

The ARE function attempts to minimize the fractional error distribution across the entire concentration range [48].

3.10.4. The hybrid fractional error function

The hybrid fractional error function (HYBRID) is given as follows:

$$\text{HYBRID} = \frac{100}{n-p} \sum_{i=1}^n \left[\frac{q_{e,\text{calc}} - q_{e,\text{exp}}}{q_{e,\text{exp}}} \right] \quad (18)$$

This error function was developed [49] to improve the fit of the ARE method at low concentration values. Instead of n as used in ARE, the sum of the fractional errors is divided by $(n-p)$, where p is the number of parameters in the isotherm equation.

3.10.5. Marquardt's percent standard deviation

Marquardt's percent standard deviation (MPSD) [50] has been used by a number of researchers in the field to test the adequacy and accuracy of the model fit with the experimental data. It has somewhat similarity to the geometric mean error distribution, but modified by incorporating the number of degrees of freedom. This error function is given as follows:

$$\text{MPSD} = 100 \sqrt{\frac{1}{n-p} \sum_{i=1}^n \left(\frac{(q_{e,\text{exp}} - q_{e,\text{calc}})}{q_{e,\text{exp}}} \right)^2} \quad (19)$$

Table 3 shows that values of these errors for the five isotherm model employed for the study.

3.11. Activation parameters

Pseudo-second-order rate constant k_s was used to calculate the activation energy E_a for biosorption of CV by EC-SDS using the Arrhenius equation [42]:

Table 3

Isotherm error analysis for adsorption of CV onto EC-SDS at different temperatures (adsorbent dose = 1 g L⁻¹, C₀ = 20 mg L⁻¹, pH = 8, equilibrium time = 100 min)

Error function	SSE	SAE	ARE	HYBRID	MPSD
303 K					
Langmuir	0.43	1.24	2.36	2.39	5.08
Freundlich	0.461	1.25	2.63	2.46	5.90
Tempkin	3.69	4.17	5.74	-1.92	8.56
Hill	20.91	10.67	15.85	-11.16	22.62
D-R	32.09	13.53	21.90	28.74	30.76
313 K					
Langmuir	0.10	0.74	1.01	-0.08	1.39
Freundlich	0.05	0.52	0.79	0.044	1.18
Tempkin	5.84	5.47	9.25	-3.92	16.64
Hill	0.11	0.75	0.98	0.02	1.36
D-R	12.03	7.96	10.29	9.49	14.59
323 K					
Langmuir	0.002	0.104	0.14	0.087	0.22
Freundlich	0.073	0.59	0.71	0.06	0.94
Tempkin	5.41	5.62	9.14	-2.40	15.12
Hill	0.002	0.10	0.14	0.008	0.20
D-R	8.10	5.94	7.29	-2.86	9.94

$$\ln k_s = \ln A - \frac{E_a}{RT} \quad (20)$$

where k_s is the pseudo-second-order rate constant, A is the Arrhenius constant, E_a is the activation energy (kJ M⁻¹), R is the gas constant (8.314 J M⁻¹ K⁻¹) and T is the temperature (K). The value of E_a (19.41 kJ M⁻¹) was obtained from the slope of linear plot of $\ln k_s$ vs. $1/T$. The magnitude of activation energy gives an idea about the type of adsorption which is mainly physical or chemical. Low activation energies (<40 kJ M⁻¹) are characteristics for physical adsorption, while higher activation energies (>40 kJ M⁻¹) suggest chemical adsorption. The activation energy obtained for the adsorption of CV onto EC-SDS indicates that the adsorption process is physical in nature.

The Eyring equation was used to calculate the standard enthalpy (ΔH^\ddagger), and entropy of activation (ΔS^\ddagger) [51]:

$$\ln \frac{k_s}{T} = \ln \frac{k_B}{h} + \frac{\Delta S^\ddagger}{R} - \frac{\Delta H^\ddagger}{RT} \quad (21)$$

where k_s is the pseudo-second-order rate constant, k_B is the Boltzman constant (1.3807×10^{-23} J K⁻¹), h is the Plank constant (6.6261×10^{-34} Js), R is the gas constant (8.314 J M⁻¹ K⁻¹), and T is the temperature (K). The values of ΔH^\ddagger and ΔS^\ddagger were calculated from the slope

and intercept of the plot of $\ln k_s/t$ vs. $1/T$ was found to be 16.81 and $-219.8 \text{ J M}^{-1} \text{ K}^{-1}$, respectively.

The values of ΔH^\ddagger and ΔS^\ddagger were used to compute the free energy of activation (ΔG^\ddagger) from the relation: $\Delta G^\ddagger = \Delta H^\ddagger - T\Delta S^\ddagger$. The value of ΔG^\ddagger at 303, 313 and 323 K are 83.40, 85.37, 87.54 kJ M^{-1} , respectively. The large positive values of ΔG^\ddagger suggest that energy was required in the biosorption reaction to convert reactants into products and hence supported the endothermic nature of the adsorption.

3.12. Thermodynamic parameters

According to thermodynamics, the Gibbs free energy change is also related to the entropy change and heat of adsorption at constant temperature. Thermodynamic parameters, that is, free energy (ΔG), enthalpy (ΔH), and entropy (ΔS) changes, were also calculated using the following thermodynamic equation and are given in Table 4.

$$\Delta G = -RT \ln K_L \quad (22)$$

$$\Delta = \Delta H - T\Delta S \quad (23)$$

From Eqs. (22) and (23), we get

$$\ln K_L = -\frac{\Delta H}{RT} + \frac{\Delta S}{R} \quad (24)$$

where ΔG , is the free energy change (kJ M^{-1}), ΔH , the change in enthalpy (kJ M^{-1}), ΔS , the entropy change ($\text{kJ M}^{-1} \text{ K}^{-1}$), T the absolute temperature (K) and R the universal gas constant ($8.314 \text{ J M}^{-1} \text{ K}^{-1}$). ΔH is determined by the slope of the linear Van't Hoff plot, $\ln K_L$ vs. $(1/T)$, using Eq. (24). The negative values of ΔG indicate the feasibility and spontaneous nature of adsorption of CV. The positive value of ΔH for EC-SDS suggests that adsorption process is endothermic in nature and increase in temperature activates the

adsorption sites. The positive values of the entropy change show the increased randomness at the solid/solution interface, with some structural changes in the adsorbate and adsorbent, and the affinity of the adsorbent for CV. When the adsorbate gets adsorbed on the surface of the adsorbents, water molecules previously bonded to the dye cation get released and dispersed in the solution; it results in an increase in the entropy [52].

4. Conclusion

This study predicts the feasibility of surface-modified *E. crassipes* as a low-cost adsorbent for the removal of dye CV. Boehm titrations, pH, pH_{zpc} measurements reveals the basic nature of the adsorbent material EC-SDS. Surface area of EC-SDS is also quite high having the value of $68.7 \text{ m}^2 \text{ g}^{-1}$. Pseudo-second-order model adequately described the adsorption process analyzed from q_e and R^2 values. The results corroborated that experimental data were correlated reasonably well by the Langmuir adsorption isotherm. Results are strengthened by statistical analysis error model. The maximum adsorption capacity for CV on EC-SDS was found to be 116.27 mg g^{-1} , respectively, which is quite high in comparison to other adsorbents. The adsorption of the dye was found to be feasible and denoted increase in randomness at interface as evidenced by ΔG and ΔS values. Mean free energy E (D-R constant) and activation energy value inferred that present adsorption process is physical in nature. Intra particle diffusion constant (k_{id}), second-order rate constant (k_s), extent of surface coverage (b), Freundlich adsorption capacity (K_F), Tempkin constant (K_T), D-R adsorption capacity constant (q_s) and Langmuir monolayer capacity (C_m) increases with increase in temperature insinuated the endothermic behavior of adsorption process. It is supported by the large positive value of free energy of activation (ΔG^\ddagger). This fact is further confirmed by the positive value of enthalpy change. The studied models demonstrated the homogenous temperature dependence of adsorption process.

Hence, the modified biomass waste shows great promise for the treatment of dye-containing wastewater as a new, low-cost, easily available and highly effective adsorbent.

Table 4

Thermodynamic parameters and R_L values for the adsorption of CV onto EC-SDS at different temperatures (adsorbent dose = 1 g L^{-1} , $C_o = 20 \text{ mg L}^{-1}$, $\text{pH} = 8$, equilibrium time = 100 min)

Temp. (K)	R_L values	$-\Delta G$ (kJ M^{-1})	ΔH (kJ M^{-1})	ΔS ($\text{JK}^{-1} \text{ M}^{-1}$)	R^2
303	0.219	28.19			
313	0.211	29.29	3.29	103.9	0.99
323	0.205	30.27			

References

- [1] S.J. Allen, K.Y.H. Khader, M. Bino, Electro oxidation of dyestuffs in waste waters, J. Chem. Technol. Biotechnol. 62 (1995) 111–117.

- [2] M. Yang, A current global view of environmental and occupational cancers, *J. Environ. Sci. Health., Part C* 29 (2011) 223–249.
- [3] D. Mohan, K.P. Singh, G. Singh, K. Kumar, Removal of dyes from wastewater using flyash, a low-cost adsorbent, *Ind. Eng. Chem. Res.* 41 (2002) 3688–3695.
- [4] O.J. Hao, H. Kim, P.C. Chiang, Decolorization of wastewater, *Crit. Rev. Env. Sci. Technol.* 30 (2000) 449–505.
- [5] R.J. Stephenson, J.B. Sheldon, Coagulation and precipitation of a mechanical pulping effluent: Removal of carbon and turbidity, *Water Res.* 30(4) (1996) 781–792.
- [6] I.A. Salem, M. El-maazawi, Kinetics and mechanism of color removal of Methylene Blue with hydrogen peroxide catalysed by some supported alumina surfaces, *Chemosphere* 41 (2000) 1173–1180.
- [7] E. Coro, S. Laha, Color removal from textile effluents using hardwood as an adsorbent, *Water Res.* 35(7) (2001) 1851–1854.
- [8] S. Wang, H. Li, L. Xu, Application of zeolite MCM-22 for basic dye removal from wastewater, *J. Colloid Interface Sci.* 295 (2006) 71–78.
- [9] A. Mittal, V. Thakur, J. Mittal, H. Vardhan, Process development for the removal of hazardous anionic azo dye congo red from wastewater by using hen feather as potential adsorbent, *Desalin. Water Treat.* (2013), doi: [10.1080/19443994.2013.785030](https://doi.org/10.1080/19443994.2013.785030).
- [10] A. Mittal, V. Thakur, V. Gajbe, Adsorptive removal of toxic azo dye amido black 10B by hen feather, *Environ. Sci. Pollut. Res.* 20 (2013) 260–269.
- [11] A. Mittal, D. Kaur, A. Malviya, J. Mittal, V.K. Gupta, Adsorption studies on the removal of coloring agent phenol red from wastewater using waste materials as adsorbents, *J. Colloid Interface Sci.* 337(2) (2009) 345–354.
- [12] A. Mittal, J. Mittal, A. Malviya, D. Kaur, V.K. Gupta, Decoloration treatment of a hazardous triarylmethane dye, Light Green SF (yellowish) by waste material adsorbents, *J. Colloid Interface Sci.* 342(2) (2010) 518–527.
- [13] A. Mittal, V.K. Gupta, Adsorptive removal and recovery of hazardous azo dye eriochrome black T, *Toxicol. Environ. Chem.* 92(10) (2010) 1813–1823.
- [14] A. Mittal, D. Jhare, J. Mittal, Adsorption of hazardous dye eosin yellow from aqueous solution onto waste material de-oiled soya: Isotherm, kinetics and bulk removal, *J. Mol. Liq.* 179 (2013) 133–140.
- [15] A. Mittal, J. Mittal, A. Malviya, V.K. Gupta, Adsorptive removal of hazardous anionic dye ‘Congo Red’ from wastewater using waste materials and recovery by desorption, *J. Colloid Interface Sci.* 340(1) (2009) 16–26.
- [16] H. Daraei, A. Mittal, M. Noorisepehr, F. Daraei, Kinetic and equilibrium studies of adsorptive removal of phenol onto eggshell waste, *Environ. Sci. Pollut. Res.* 20 (2013) 4603–4611.
- [17] A. Mittal, D. Jhare, J. Mittal, V.K. Gupta, Batch and bulk removal of hazardous colouring agent Rose Bengal by adsorption over bottom ash, *RSC Adv.* 2 (22) (2012) 8381–8389.
- [18] A. Mittal, R. Jain, S. Varshney, S. Sikarwar, J. Mittal, Removal of Yellow ME 7 GL from industrial effluent using electrochemical and adsorption techniques, *Int. J. Env. Poll.* 43(4) (2010) 308–323.
- [19] J. Mittal, V. Thakur, A. Mittal, Batch removal of hazardous azo dye bismark brown R using waste material hen feather, *Ecol. Eng.* 60 (2013) 249–253.
- [20] A. Mittal, V.K. Gupta, A. Malviya, J. Mittal, Process development for the batch and bulk removal and recovery of a hazardous, water-soluble azo dye (metanil yellow) by adsorption over waste materials (Bottom ash and de-oiled soya), *J. Hazard. Mater.* 151 (2–3) (2008) 821–832.
- [21] V.K. Gupta, Suhas, Application of low-cost adsorbents for dye removal—A review, *J. Environ. Manage.* 90 (2009) 2313–2342.
- [22] I. Eiichi, T. Ogawa, T.C. Yatome, H. Horisu, Behavior of activated sludge with dyes, *Bull. Environ. Contam. Toxicol.* 35 (1985) 729–734.
- [23] C. Sahoo, A.K. Gupta, A. Pal, Photocatalytic degradation of Crystal violet (C.I. Crystal violet) on silver ion doped TiO₂, *Dyes Pigm.* 66 (2005) 189–196.
- [24] J.J. Jone, J.O. Falkinham III, Decolorization of malachite green and crystal violet by waterborne pathogenic mycobacteria, *Antimicrob. Agents Chemother.* 47 (2003) 2323–2326.
- [25] A. Mittal, J. Mittal, A. Malviya, D. Kaur, V.K. Gupta, Adsorption of hazardous dye crystal violet from wastewater by waste materials, *J. Colloid Interface Sci.* 343 (2010) 463–473.
- [26] L. Lachman, H.A. Lieberman, J.L. Kanig, *The Theory and Practice of Industrial Pharmacy*, 3rd Indian ed., Varghese publishing house (Copyright Lea & Febiger USA), Bombay, 1987, p. 27.
- [27] J. Rivera-Utrilla, I. Bautista-Toledo, M.A. Ferro-Garcia, C. Moreno-Castilla, Activated carbon surface modifications by adsorption of bacteria and their effect on aqueous lead adsorption, *J. Chem. Technol. Biotechnol.* 76 (2001) 1209–1215.
- [28] H.P. Boehm, Some aspects of the surface chemistry of carbon blacks and other carbons, *Carbon* 32 (1994) 759–769.
- [29] A. Witek-Krowiak, Biosorption of malachite green from aqueous solutions by pine sawdust: Equilibrium, kinetics and the effect of process parameters, *Desalin. Water Treat.* 51 (2013) 3284–3294.
- [30] M. Alkan, M. Dogan, Adsorption of copper (II) onto perlite, *J. Colloid Interface Sci.* 243 (2001) 280–291.
- [31] G. Alberghina, R. Bianchini, M. Fichera, S. Fisichella, Dimerization of cibacron blue F3GA and other dyes: Influence of salts and temperature, *Dyes Pigm.* 46 (2000) 129–137.
- [32] X. Peng, Z. Luan, H. Zhang, Montmorillonite-Cu(II)/Fe(III) oxides magnetic material as adsorbent for removal of humic acid and its thermal regeneration, *Chemosphere* 63 (2006) 300–306.
- [33] W.J. Weber, J.C. Morris, Kinetics of adsorption on carbon from solution, *J. Sanit. Eng. Div. ASCE* 89 (1963) 31–60.
- [34] S.J. Allen, G. Mckay, K.Y.H. Khader, Intraparticle diffusion of a basic dye during adsorption on to sphagnum peat, *Environ. Pollut.* 56 (1989) 39–50.
- [35] C. Gerente, V.K.C. Lee, P. Le Cloirec, G. Mckay, Application of chitosan for the removal of metals from wastewaters by adsorption-mechanisms and models-review, *Crit. Rev. Env. Sci. Technol.* 37 (2007) 41–127.

- [36] C. Aharoni, S. Sideman, E. Hoffer, Adsorption of phosphate ions by colloid ion—Coated alumina, *J. Chem. Technol. Biotechnol.* 29 (1979) 404–412.
- [37] E. Tutem, R. Apak, C.F. Unal, Adsorptive removal of chlorophenols from water by bituminous shale, *Water Res.* 32 (1998) 2315–2324.
- [38] G.E. Boyd, A.W. Adamson, L.S. Meyers, The exchange adsorption of ions from aqueous solution by organic zeolites II kinetics, *J. Am. Chem. Soc.* 69 (1947) 2836–2848.
- [39] D. Reichenberg, Properties of ion exchange resins in relation to their structure. III. Kinetics of exchange, *J. Am. Chem. Soc.* 75 (1953) 589–597.
- [40] J. Mittal, D. Jhare, H. Vardhan, A. Mittal, Utilization of bottom ash as a low-cost sorbent for the removal and recovery of a toxic halogen containing dye Eosin Yellow, *Desalin. Water Treat.* (2013), doi: [10.1080/19443994.2013.803265](https://doi.org/10.1080/19443994.2013.803265).
- [41] S. Sumanjit, R.K. Rani, Mahajan, Adsorptive removal of dye crystal violet onto low-cost carbon produced from Eichhornia plant: Kinetic, equilibrium, and thermodynamic studies, *Desalin. Water Treat.* (2013), doi: [10.1080/19443994.2013.841109](https://doi.org/10.1080/19443994.2013.841109).
- [42] G. Crini, Kinetic and equilibrium studies on the removal of cationic dyes from aqueous solution by adsorption onto a cyclodextrin polymer, *Dyes Pigm.* 77 (2008) 415–426.
- [43] M. Yurtsever, I.A. Sengil, Biosorption of Pb(II) ions by modified quebracho tannin resin, *J. Hazard. Mater.* 163 (2009) 58–64.
- [44] D. Ringot, B. Lerzy, K. Chaplain, J.P. Bonhoure, E. Auclair, Y. Larondelle, *In vitro* biosorption of ochratoxin A on the yeast industry by-products: Comparison of isotherm models, *Bioresour. Technol.* 98 (2007) 1812–1821.
- [45] L.K. Koopal, W.H. Van Riemsdijk, D.G. Kinniburgh, Humic matter and contaminants. General aspects and modelling ion binding, *Pure Appl. Chem.* 73 (2001) 2005–2016.
- [46] O. Gercel, H.F. Gercel, A.S. Kopal, U.B. Ogutveren, Removal of disperse dye from aqueous solution by novel adsorbent prepared from biomass plant material, *J. Hazard. Mater.* 160 (2008) 668–674.
- [47] R.K. Rajoriya, B. Prasad, I.M. Mishra, K.L. Wasewar, Adsorption of benzaldehyde on granular activated carbon: Kinetics, equilibrium, and thermodynamic, *Chem. Biochem. Eng. Q.* 21(3) (2007) 219–226.
- [48] A. Kapoor, R.T. Yang, Correlation of equilibrium adsorption data of condensable vapours on porous adsorbents, *Gas Sep. Purif.* 3(4) (1989) 187–192.
- [49] J.F. Porter, G. McKay, K.H. Choy, The prediction of sorption from a binary mixture of acidic dyes using single- and mixed-isotherm variants of the ideal adsorbed solute theory, *Chem. Eng. Sci.* 54 (1999) 5863–5885.
- [50] S. Chowdhury, P. Saha, Adsorption kinetic modeling of safranin onto rice husk biomatrix using pseudo-first- and pseudo second-order kinetic models: Comparison of linear and non-linear method, *Clean—Soil, Air Water* 39(3) (2011) 274–282.
- [51] S. Chakraborty, S. Chowdhury, P.D. Saha, Adsorption of crystal violet from aqueous solution onto NaOH-modified rice husk, *Carbohydr. Polym.* 86 (2011) 1533–1541.
- [52] S. Senthilkumar, P. Kalaamani, C.V. Subburaam, Liquid phase adsorption of crystal violet onto activated carbons derived from male flowers of coconut tree, *J. Hazard. Mater.* B136 (2006) 800–808.